ChemComm

COMMUNICATION

View Article Online
View Journal | View Issue

Cite this: *Chem. Commun.*, 2023, 59, 11811

Received 31st August 2023,
Accepted 12th September 2023

DOI: 10.1039/d3cc04291j

rsc.li/chemcomm

Binding modes of high stoichiometry guest complexes with a Co_8L_{12} cage uncovered by mass spectrometry†

Daniel L. Stares, ‡[a] Cristina Mozaceanu,‡[b] Michael D. Ward *[b] and Christoph A. Schalley *[a]

We demonstrate how different modes of guest binding with a Co_8L_{12} cubic cage can be determined using ESI-MS. High stoichiometry guest binding was observed, with the guests preferentially binding externally, but internal guest inclusion was also seen at higher guest loading.

Self-assembled metal–organic cages are some of the most sophisticated and complex synthetic host structures.[1,2] Characterisation of these hosts typically relies on either NMR or X-ray crystallography with it being less common to utilise mass spectrometry (MS) for structural analysis. MS has the general benefits that an ion of interest can be mass-selected, so it does not require completely pure samples; it is highly sensitive and data can be obtained relatively quickly.[3] For self-assembled systems more specifically, MS has the added advantage that it deals with isolated ions, free from any competitive solvent, and as such, any dynamic exchange processes which can complicate characterisation in solution are absent.[4] Because of this, the mass-to-charge ratio (m/z) of an ion easily furnishes a system's stoichiometry which can be especially useful when studying host–guest systems capable of binding multiple guest molecules.[5,6] Beyond stoichiometry, structural information such as guest binding mode can be gained through tandem MS techniques such as ion-mobility mass spectrometry (IMS) and collision-induced dissociation (CID).[7–10] IMS separates ions based on their size and can thus distinguish isomers that vary due to different isomeric ligands, guest binding position and even diastereomeric composition of the cage.[11–15] CID is a dissociation technique, where ions are collided with a neutral buffer gas to induce fragmentation and can be used to probe structural features of the cage as well as guest binding modes.[16–18]

The Co_8L_{12} cubic cage ($\mathbf{H^W_{Co}}$) (Fig. 1), based on hydroxymethyl-substituted bis-bidentate ligands ($\mathbf{L^W}$) which span the edges of an approximately cubic array of Co(II) ions, can bind guests internally and externally and is also capable of binding multiple guests.[19–22] However, multiple guest binding has only been demonstrated using X-ray crystallography and NMR spectroscopy under forcing conditions with a large excess of guest.[19–21] Detailed MS studies, which are well suited to studying higher stoichiometry guest binding, have currently not been performed. Herein, a combination of IMS and CID experiments were used to investigate the host–guest properties of $\mathbf{H^W_{Co}}$, particularly to uncover its multiple guest binding capabilities. The results serve as a further case study of the benefit of MS in the study of host–guest chemistry of metal–organic cages especially by allowing observation of different binding modes.

$\mathbf{H^W_{Co}}$ ionises through loss of BF_4^- counterions generating charge states from 5+ to 10+ (Fig. 2). Additionally, some

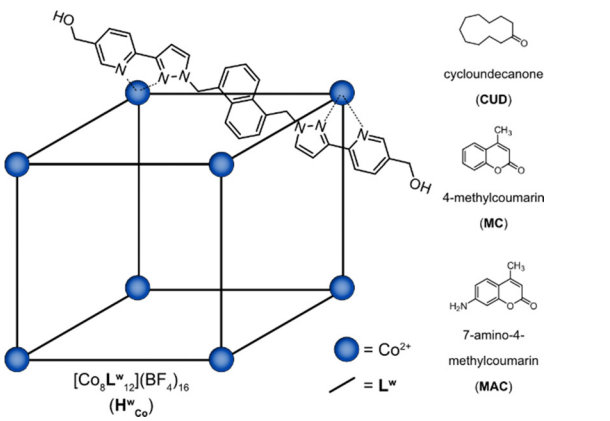

Fig. 1 Structure of the $\mathbf{H^W_{Co}}$ cage and the guests used in the current study.

[a] *Institut für Chemie und Biochemie, Freie Universität Berlin, Arnimallee 20, Berlin, 14195, Germany. E-mail: c.schalley@fu-berlin.de*
[b] *Department of Chemistry, University of Warwick, Coventry CV4 7AL, UK. E-mail: m.d.ward@warwick.ac.uk*

† Electronic supplementary information (ESI) available: Sample preparation, instrumental parameters, computational details and additional figures. See DOI: https://doi.org/10.1039/d3cc04291j

‡ Authors contributed equally.

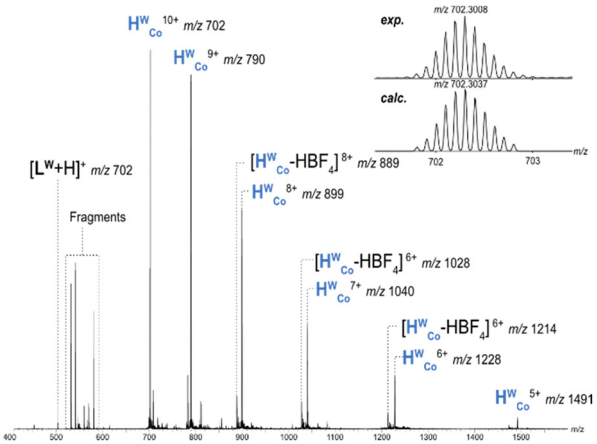

Fig. 2 ESI-MS spectrum of 10 μM $\mathbf{H^W_{Co}}$ in H_2O, the 10+ to 5+ cage charge states are marked. Fragmentation products and cage species resulting from the loss of HBF_4 are also observed. The experimental *vs.* calculated *m/z* values for $\mathbf{H^W_{Co}}^{10+}$ are shown in the inset.

fragment ions were present and a loss of neutral HBF_4 (likely as HF and BF_3) was also observed for charge states 5+ to 9+. The charge state distribution could be shifted towards higher charges by increasing the capillary voltage, but cage fragmentation became more pronounced and charge states over 10+ were still not observed (Fig. S1, ESI†). This indicates that charge states over 10+ are not stable enough to survive in the instrument with the six counterions necessary to counterbalance the charge repulsion within the cage. X-ray crystal structures of $\mathbf{H^W_{Co}}$ show discrete binding of six counterions in the portals of the faces which will significantly reduce charge repulsion of the cage as these counterions are surrounded by four metal centres and their respective charges.[23,24] The removal of these six counterions during ionisation would thus be more difficult than peripherally bound ones requiring higher capillary voltages to do so, and, if successfully removed, would lead to significant destabilisation.[25] The interplay of these two factors can explain why charge states greater than 10+ are not observed. CID of the cage showed fragmentation into face, corner and edge fragments, (Fig. S2 and S3, ESI†) but overall, the cage is relatively stable, considering the charge state, with $\mathbf{H^W_{Co}}^{10+}$ surviving until a collision voltage of 8 V (Fig. S4, ESI†).

The host–guest chemistry of $\mathbf{H^W_{Co}}$ was then explored with guests whose binding has been studied in solution and the solid state: cycloundecanone (**CUD**); 4-methylcoumarin (**MC**); and 7-amino-4-methylcoumarin (**MAC**) (Fig. 1). **CUD** has been shown to bind strongly inside the cavity of $\mathbf{H^W_{Co}}$ in water driven by the hydrophobic effect with a 1 : 1 $\mathbf{H^W_{Co}}$**/CUD** stoichiometry.[26] In contrast, it has been shown that multiple guest binding is possible when **MC** and **MAC** are used as guests.[19] Accordingly, a 1 : 1 $\mathbf{H^W_{Co}}$**/CUD** complex was observed in the mass spectrum with no evidence of multiple guests binding (Fig. S5, ESI†) whilst for **MC**, small signals for the 1 : 2 complex were seen in addition to the 1 : 1 $\mathbf{H^W_{Co}}$**/MC** complex (Fig. S6, ESI†). With **MAC**, strong signals were observed for $\mathbf{H^W_{Co}}$/(1–4)**MAC** complexes with even higher host:guest stoichiometries also seen albeit at lower signal intensities (Fig. 3a and Fig. S7, ESI†). The results for **CUD** and **MC** are consistent with what has previously been observed in solution and the solid state but the higher stoichiometries associated with **MAC** binding are observed for the first time.

For all three guests, CID of the 1 : 1 $\mathbf{H^W_{Co}}$**/Guest (G)**$^{8+}$ species resulted in complete guest loss to the free $\mathbf{H^W_{Co}}^{8+}$ at low collision voltages before further fragmentation of $\mathbf{H^W_{Co}}^{8+}$ as seen for the free cage (Fig. S3, S4 and S8–S10, ESI†). Although a lower charge state was mass-selected to reduce Coulomb repulsion and instrument conditions were softened as much as

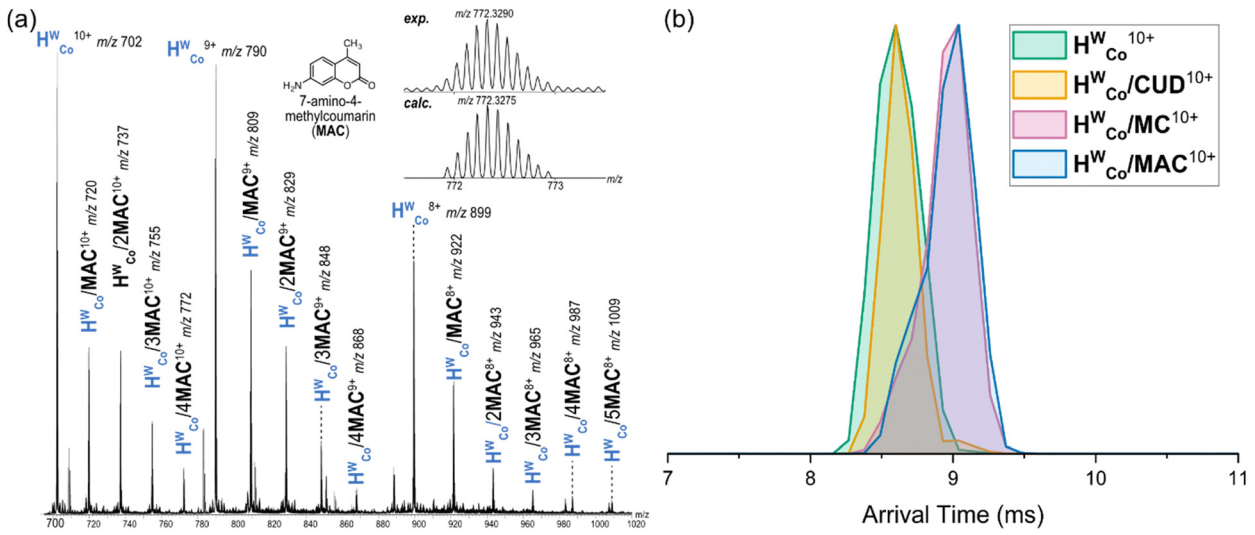

Fig. 3 (a) ESI-HRMS spectrum of $\mathbf{H^W_{Co}}$ with **MAC** (10 μM/50 μM) in 5% CH_3OH/H_2O. Multiple guest binding stoichiometries with up to 5 **MAC**s bound are observed. The experimental *vs.* calculated *m/z* values for the $\mathbf{H^W_{Co}}$/4**MAC**$^{10+}$ are shown in the inset (b) ATDs of $\mathbf{H^W_{Co}}^{10+}$, $\mathbf{H^W_{Co}}$**/CUD**$^{10+}$, $\mathbf{H^W_{Co}}$**/MC**$^{10+}$, $\mathbf{H^W_{Co}}$**/MAC**$^{10+}$. The ATDs of $\mathbf{H^W_{Co}}^{10+}$ and $\mathbf{H^W_{Co}}$**/CUD**$^{10+}$ overlap indicating encapsulation whilst $\mathbf{H^W_{Co}}$**/MC**$^{10+}$ and $\mathbf{H^W_{Co}}$**/MAC**$^{10+}$ have longer arrival times consistent with external binding.

possible, a portion of empty cage was still observed after mass selection of $\mathbf{H^W_{Co}/G}^{8+}$ ions without additional collision voltages applied. This means that some guest dissociation can occur just from transmission through the instrument. The relative intensities of $\mathbf{H^W_{Co}/CUD}^{8+}$ and $\mathbf{H^W_{Co}/MAC}^{8+}$ (71 and 77%, respectively) after mass selection are considerably higher than that for $\mathbf{H^W_{Co}/MC}^{8+}$ (47%) meaning that higher proportions of the **CUD** and **MAC** complexes survive transmission though the instrument (Fig. S11, ESI†). Complete guest loss was observed at low collision voltages with all guests but as the $\mathbf{H^W_{Co}/G}$ complexes do not represent 100% of the total intensity after mass selection, it is not possible to complete a full survival yield analysis to determine relative stabilities of the guests. Thus, no reasonable conclusion about the stabilities of the host:guest complexes can be drawn other than that all three guests are lost at similar collision voltages.

IMS of the different 1 : 1 $\mathbf{H^W_{Co}/G}$ complexes showed comparable arrival times for $\mathbf{H^W_{Co}}^{10+}$ and $\mathbf{H^W_{Co}/CUD}^{10+}$ with longer arrival times for $\mathbf{H^W_{Co}/MC}^{10+}$ and $\mathbf{H^W_{Co}/MAC}^{10+}$ (Fig. 3b). A straightforward explanation of these results is that **CUD** is encapsulated in the central cavity of $\mathbf{H^W_{Co}}$ as seen in crystal structures,[26] and hence does not contribute significantly to the collisional cross section (CCS) of the cage ion, whereas both **MC** and **MAC** are bound to the external cage surface increasing the CCS and hence arrival times. Although a comparison of absolute CCS values is difficult due to a lack of suitable calibrants and issues with the theoretical calculations for metal–organic complexes,[27] relative comparisons of theoretical CCS values are still insightful as any errors cancel each other out. Here, theoretical CCS values using the trajectory method ($^{TM}CCS_{N2}$) were calculated for universal force field (UFF) optimised structures of $\mathbf{H^W_{Co}}^{10+}$ and $\mathbf{H^W_{Co}/G}^{10+}$ with the different guests.[28,29] They supported the above assessment by showing the same general results as the IMS with very similar $^{TM}CCS_{N2}$ values for $\mathbf{H^W_{Co}}^{10+}$ and $\mathbf{H^W_{Co}/CUD}^{10+}$ when the **CUD** was encapsulated; with increases in the $^{TM}CCS_{N2}$ values of $\mathbf{H^W_{Co}/MC}^{10+}$ and $\mathbf{H^W_{Co}/MAC}^{10+}$ with **MAC** and **MC** binding externally *via* hydrogen bonding with $\mathbf{L^W}$ (Fig. S12, ESI†). Thus, the IMS experiments strongly support encapsulation of **CUD** in the host cavity, with external binding of **MAC** and **MC** for the 1 : 1 stoichiometries.

Encapsulation of **CUD** in solution is driven by the hydrophobic effect which is not present in the gas-phase and thus **CUD** complexes may be expected to not be observed *via* MS. However, **CUD** is capable of =O···H–C hydrogen bonds in the *fac* tris-chelate pocket of the cavity and guest loss would also be partially prevented by the counterions in the face-portals increasing the dissociation barrier and enabling a significant amount of the **CUD** complex to survive after ionisation.[26] External binding of **MC** likely involves =O···H–O hydrogen bonds with the hydroxy groups of $\mathbf{L^W}$. Compared to **MC**, the presence of the aniline in **MAC** would enable it to form an additional O–H···NH_2 hydrogen bond with the corner of the cage. Computational models at the B97-3c level of theory implemented in the Orca program shows that both *mer* and *fac* corner units of $\mathbf{H^W_{Co}}$ are ideally suited to accommodate two

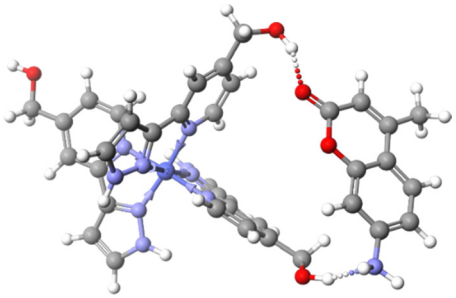

Fig. 4 Binding mode of **MAC** with two $\mathbf{L^W}$ in a *mer* tris-chelate corner of $\mathbf{H^W_{Co}}$. Structure was optimised at the B97-3c level of theory.

hydrogen bonds with **MAC** (Fig. 4 and Fig. S13, ESI†).[30–32] The aniline might also enable ion pairing by deprotonating the OH to give R–$NH_3^+\cdots{}^-$O–R′ interactions. These additional interactions available to **MAC** could potentially explain the higher stoichiometry complexes not observed for the other guests. Furthermore, the binding modes of **MC** and **MAC** *via* hydrogen bonding with the cage exterior also justify the difficulty in observing the complexes in solution as those measurements are performed in competitive solvents such as H_2O where cavity binding dominates due to the hydrophobic effect.[19]

The arrival time distributions (ATD) of the $\mathbf{H^W_{Co}}/n\mathbf{MAC}^{10+}$ complexes show increasing arrival times with increasing *n* but also show shoulder regions at earlier arrival times which increase in magnitude with additional **MAC**s until clear double peaks are seen in the ATDs of $\mathbf{H^W_{Co}}/3\mathbf{MAC}^{10+}$ and $\mathbf{H^W_{Co}}/4\mathbf{MAC}^{10+}$ (Fig. 5a). This can be explained by two concurrent binding modes: one where all **MAC** are bound externally and the other where one **MAC** has been encapsulated. The increasing proportion of encapsulated **MAC** at higher guest loading indicates that it preferentially binds externally but at high enough guest loading, probability will dictate that one will be encapsulated. The ATDs show that the contribution coming from the binding mode with one **MAC** encapsulated is slightly larger than the lower stoichiometry with all guests bound externally (*e.g.* $\mathbf{H^W_{Co}}/3\mathbf{MAC}^{10+}$ with one **MAC** encapsulated is slightly larger than the $\mathbf{H^W_{Co}}/2\mathbf{MAC}^{10+}$ with all **MAC** bound externally), whereas $\mathbf{H^W_{Co}}^{10+}$ and $\mathbf{H^W_{Co}/CUD}^{10+}$ overlap (Fig. 3b). This could reflect the better fit of the conformationally flexible **CUD**, whereas encapsulation of the more rigid **MAC** and **MC** likely leads to some expansion of the cage which is reflected in the longer arrival times.

It should be noted that due to the facile guest loss, the observed ions could well be derived from higher guest stoichiometry complexes which have subsequently undergone guest loss in the instrument. Energy-resolved IMS can study this by performing CID in the trap cell prior to IMS and monitoring the changes in the ATDs allowing an assessment of the stability of different binding modes.[33] Measurements with mass selected $\mathbf{H^W_{Co}}/4\mathbf{MAC}^{10+}$ led to dissociation of **MAC** to form $\mathbf{H^W_{Co}}/3\mathbf{MAC}^{10+}$. When comparing the ATD of the 'free' $\mathbf{H^W_{Co}}/3\mathbf{MAC}^{10+}$ (mass selected from full spectrum) it showed that the $\mathbf{H^W_{Co}}/3\mathbf{MAC}^{10+}$ formed purely from dissociation of the $\mathbf{H^W_{Co}}/4\mathbf{MAC}^{10+}$ only had one major contribution in the ATD which

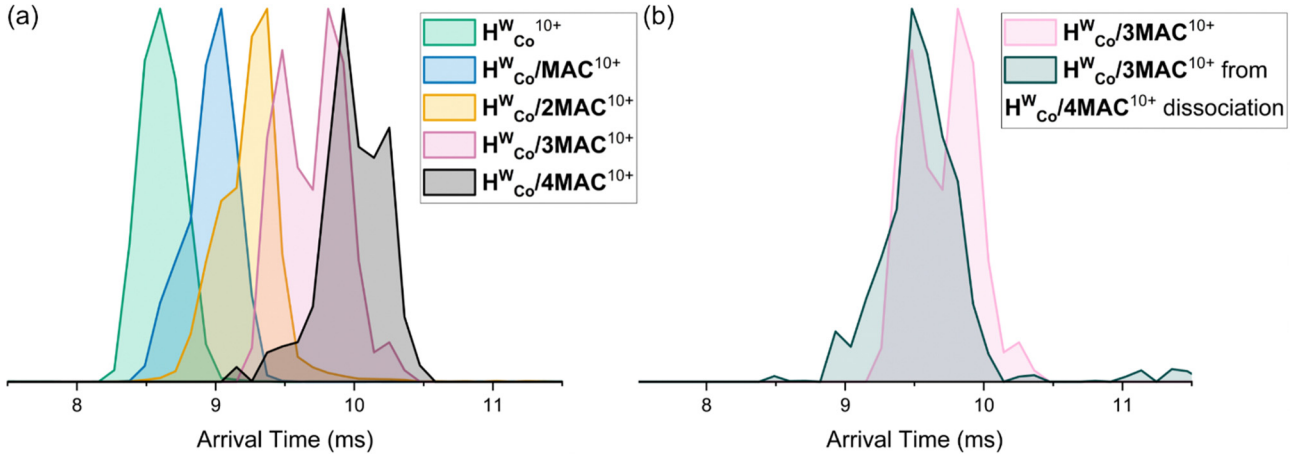

Fig. 5 (a) ATDs of $H^{W}_{Co}/nMAC^{10+}$ with n = 1–4. (b) ATDs of 'free' $H^{W}_{Co}/3MAC^{10+}$ and $H^{W}_{Co}/3MAC^{10+}$ formed purely from dissociation of $H^{W}_{Co}/4MAC^{10+}$.

correlated to the earlier contribution of that of the 'free' $H^{W}_{Co}/3MAC^{10+}$ (Fig. 5b). This means that externally bound guests dissociate more easily than internally bound ones even though encapsulation occurs less readily.

In conclusion, the MS techniques of IMS and CID were used to study a Co_8L_{12} cubic cage and its host–guest properties with three different guests. The studies demonstrated a major stabilising effect of the counterions binding in the faces of the portals. The host–guest properties of the cage showed that guests had different preferences for external or internal binding. Higher stoichiometries of guest binding, which have not been seen with other techniques, were observed and investigated. These showed that **MAC** preferentially binds externally but could also be driven inside the cavity at high guest loading. These results demonstrate the ability of MS to investigate metal–organic hosts and probe guest binding modes.

We thank the European Union through the NOAH project (H2020-MSCA-ITN project Ref. 765297) and FU Berlin for funding. Support for measurements by the BioSupraMol core facility at FU Berlin is gratefully acknowledged. Thank you to those at Warwick for help with cage synthesis.

Conflicts of interest

There are no conflicts to declare.

Notes and references

1 F. J. Rizzuto, L. K. S. von Krbek and J. R. Nitschke, *Nat. Rev. Chem.*, 2019, **3**, 204–222.
2 D. Fujita, Y. Ueda, S. Sato, N. Mizuno, T. Kumasaka and M. Fujita, *Nature*, 2016, **540**, 563–566.
3 C. A. Schalley, *Mass Spectrom. Rev.*, 2001, **20**, 253–309.
4 Z. Qi, T. Heinrich, S. Moorthy and C. A. Schalley, *Chem. Soc. Rev.*, 2015, **44**, 515–531.
5 A. J. McConnell, *Chem. Soc. Rev.*, 2022, **51**, 2957–2971.
6 W. Meng, B. Breiner, K. Rissanen, J. D. Thoburn, J. K. Clegg and J. R. Nitschke, *Angew. Chem., Int. Ed.*, 2011, **50**, 3479–3483.
7 H. Wang, C. Guo and X. Li, *CCS Chem.*, 2021, **4**, 785–808.
8 E. Kalenius, M. Groessl and K. Rissanen, *Nat. Rev. Chem.*, 2019, **3**, 4–14.
9 C. Vicent, V. Martinez-Agramunt, V. Gandhi, C. Larriba-Andaluz, D. G. Gusev and E. Peris, *Angew. Chem., Int. Ed.*, 2021, **60**, 15412–15417.
10 K. J. Endres, K. Barthelmes, A. Winter, R. Antolovich, U. S. Schubert and C. Wesdemiotis, *Rapid Commun. Mass Spectrom.*, 2020, **34**, e8717.
11 K. E. Ebbert, L. Schneider, A. Platzek, C. Drechsler, B. Chen, R. Rudolf and G. H. Clever, *Dalton Trans.*, 2019, **48**, 11070–11075.
12 G. Carroy, V. Lemaur, C. Henoumont, S. Laurent, J. De Winter, E. De Pauw, J. Cornil and P. Gerbaux, *J. Am. Soc. Mass Spectrom.*, 2018, **29**, 121–132.
13 H. Lee, J. Tessarolo, D. Langbehn, A. Baksi, R. Herges and G. H. Clever, *J. Am. Chem. Soc.*, 2022, **144**, 3099–3105.
14 T. R. Schulte, J. J. Holstein and G. H. Clever, *Angew. Chem., Int. Ed.*, 2019, **58**, 5562–5566.
15 M. C. Pfrunder, D. L. Marshall, B. L. J. Poad, E. G. Stovell, B. I. Loomans, J. P. Blinco, S. J. Blanksby, J. C. McMurtrie and K. M. Mullen, *Angew. Chem., Int. Ed.*, 2022, **61**, e202212710.
16 E. Taipale, J. S. Ward, G. Fiorini, D. L. Stares, C. A. Schalley and K. Rissanen, *Inorg. Chem. Front.*, 2022, **9**, 2231–2239.
17 L. Sleno and D. A. Volmer, *J. Mass Spectrom.*, 2004, **39**, 1091–1112.
18 S. Ibáñez, C. Vicent and E. Peris, *Angew. Chem., Int. Ed.*, 2022, **61**, e202112513.
19 C. G. P. Taylor, S. P. Argent, M. D. Ludden, J. R. Piper, C. Mozaceanu, S. A. Barnett and M. D. Ward, *Chem. – Eur. J.*, 2020, **26**, 3054–3064.
20 C. Mozaceanu, C. G. Taylor, J. R. Piper, S. P. Argent and M. D. Ward, *Chemistry*, 2020, **2**, 22–32.
21 C. G. Taylor, J. S. Train and M. D. Ward, *Chemistry*, 2020, **2**, 510–524.
22 C. Mozaceanu, A. B. Solea, C. G. P. Taylor, B. Sudittapong and M. D. Ward, *Dalton Trans.*, 2022, **51**, 15263–15272.
23 W. Cullen, M. C. Misuraca, C. A. Hunter, N. H. Williams and M. D. Ward, *Nat. Chem.*, 2016, **8**, 231–236.
24 M. D. Ward, C. A. Hunter and N. H. Williams, *Acc. Chem. Res.*, 2018, **51**, 2073–2082.
25 B. Hasenknopf, J.-M. Lehn, B. O. Kneisel, G. Baum and D. Fenske, *Angew. Chem., Int. Ed. Engl.*, 1996, **35**, 1838–1840.
26 S. Turega, W. Cullen, M. Whitehead, C. A. Hunter and M. D. Ward, *J. Am. Chem. Soc.*, 2014, **136**, 8475–8483.
27 N. Geue, T. S. Bennett, A.-A.-M. Arama, L. A. I. Ramakers, G. F. S. Whitehead, G. A. Timco, P. B. Armentrout, E. J. L. McInnes, N. A. Burton, R. E. P. Winpenny and P. E. Barran, *J. Am. Chem. Soc.*, 2022, **144**, 22528–22539.
28 V. Shrivastav, M. Nahin, C. J. Hogan and C. Larriba-Andaluz, *J. Am. Soc. Mass Spectrom.*, 2017, **28**, 1540–1551.
29 A. K. Rappé, C. J. Casewit, K. Colwell, W. A. Goddard and W. M. Skiff, *J. Am. Chem. Soc.*, 1992, **114**, 10024–10035.
30 J. G. Brandenburg, C. Bannwarth, A. Hansen and S. Grimme, *J. Chem. Phys.*, 2018, **148**, 064104.
31 F. Neese, *Wiley Interdiscip. Rev.: Comput. Mol. Sci.*, 2012, **2**, 73–78.
32 F. Neese, *Wiley Interdiscip. Rev.: Comput. Mol. Sci.*, 2022, **12**, e1606.
33 X. Li, Y.-T. Chan, G. R. Newkome and C. Wesdemiotis, *Anal. Chem.*, 2011, **83**, 1284–1290.